Available online at www.sciencedirect.com
SCIENCE DIRECT®
International Journal of Mass Spectrometry 233 (2004) 173–179
International Journal of Mass Spectrometry
www.elsevier.com/locate/ijms

# Charge driven fragmentation of biologically relevant molecules

T. Schlathölter*, R. Hoekstra, R. Morgenstern

*KVI Atomic Physics, Rijksuniversiteit Groningen, Zernikelaan 25, 9747AA Groningen, The Netherlands*

Received 30 September 2003; accepted 21 December 2003

**Abstract**

A highly charged ion causes ultrastrong electric fields at the location of a close-by target molecule. As a response to those fields, several electrons are removed from the molecule on a very short time-scale. In the subsequent fragmentation process, ions with kinetic energies of a few hundred electron volts are produced. We investigated the interaction of 0.5 MeV $Xe^{25+}$ with the nucleobases uracil and thymine by means of coincidence time-of-flight spectrometry. Our measurements clearly show that fragment kinetic energies reflect the molecular geometry and contain information on the fragmentation pathways.


*Keywords:* Nucleobases; Highly charged ions; Time-of-flight spectrometry

## 1. Introduction

The interaction of ionizing radiation (e.g., α-, β-, and γ-rays) with biological tissue can induce severe damage to DNA. It is now generally believed that this damage is mainly due to single and double strand breaks of DNA and clustered lesions [1]. About two-thirds of this damage are not due to the primary radiation itself but due to secondary particles generated along the track [2]. These secondary particles include low energy electrons, radicals as well as singly and multiply charged ions. It is the interaction of these secondary particles with biologically relevant molecules, which is responsible for a large fraction of the action.

In this context, in particular, the interaction of low energy electrons with biologically relevant molecules has been studied. Boudaiffa et al. [3] showed that electrons between 3 and 20 eV can induce single and double strand breaks in supercoiled DNA. Other studies focused on the interaction of low energy electrons with DNA bases [4], the RNA base uracil [5] as well as bromouracil [6]. In a very recent experiment Märk and coworkers [7] investigated the interaction of subexcitation energy electrons (<3 eV) with gas-phase nucleobases uracil, thymine and cytosine [8] and observed dissociative electron attachment only. The main channel was found to be hydrogen radical abstraction, suggesting the likeliness of major biological damage inflicted by the very many secondary electrons of such low energies.

Multiply charged ions (MCI) as secondary particles are formed for instance by core ionization of heavier atoms in biological tissue and subsequent Auger-deexcitation. However, MCI also play an important role as primary particles in biological radiation damage, e.g., in heavy ion cancer therapy [9] or exposure of astronauts to the heavily charged fraction of cosmic radiation [10]. Here, most of the damage occurs when the MCI are slowed down to MeV energies and below, where the ion velocity becomes comparable to the velocities of electrons inside an atom.

In a recent study on keV $C^{q+}$ interaction with uracil we oberved a strong influence of the $C^{q+}$ ($q = 1$–6) electronic structure on the ionization and fragmentation process. Only for $C^{2+}$ almost complete fragmentation occurs whereas for all other projectile charge states the induced fragment yield is much lower. Furthermore, no single atom abstraction from the molecule was observed but rather complete shattering of the ring [11]. Coincidence studies of thymine fragments after interaction with $C^{q+}$ ions revealed a strong dependence of the fragment kinetic energies on the fragments initial location within the parent molecule [12]. It was also found that the fragmentation process for both nucleobases can be divided into three regimes: (i) non-dissociative ionization; (ii) multi-fragmentation and (iii) two-body breakup [13].

By studying the interaction of $Xe^{q+}$ ($q = 5$–25) with nucleobases we extended our studies to the regime of

* Corresponding author.
*E-mail address:* tschlat@kvi.nl (T. Schlathölter).
*URL:* http://www.kvi.nl/atf/.

1387-3806/$ – see front matter © 2004 Elsevier B.V. All rights reserved.
doi:10.1016/j.ijms.2003.12.029

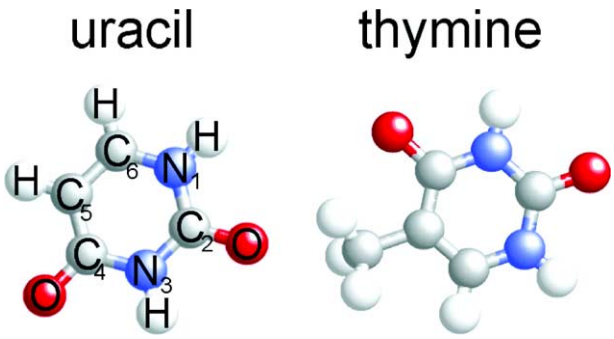


Fig. 1. Sketch of the nucleobases uracil and thymine.

fragmentation induced by ultrastrong electric fields [14]. The energies of singly charged fragments were found to exceed 100 eV. The fragment kinetic energies were also found to strongly reflect the molecular geometry.

The molecules under study here, uracil and thymine, are sketched in Fig. 1. Essentially they have benzene like structure with the C atoms at position 1′and 3′replaced by N atoms. Two of the benzene H atoms are replaced by O, respectively and, in case of thymine another H atom is replaced by a methyl group.

In the following we will discuss the issue of ultrastrong electric field induced fragmentation with a focus on the formation of multiply charged fragment ions. The experimental results will then be compared with a Coulomb explosion model.

## 2. Experiment

The electron cyclotron resonance ion source at the KVI in Groningen is used to generate $^{129}Xe^{25+}$. A source potential of 20 kV is chosen, leading to projectile ion velocities of ≈ 0.4 a.u. A 110°magnet is used for $m/q$ separation. Quadrupole magnet triplets and bending magnets guide the projectile ion beam into the experimental setup.

A sketch of the setup can be found in Fig. 2. In the setup, the ion beam is collimated by means of two 1 mm diaphragms (205 mm apart) and focussed into the collision region. The uracil or thymine gaseous target is produced by evaporation from a powder sample in a resistively heated oven. Oven temperatures of 180°(uracil) and 170°(thymine) ensure sufficient target densities without thermal dissociation of the molecules. A 500 μm nozzle placed ≈20 mm from the collision region limits the contamination of the vacuum chamber. A liquid nitrogen cooled stainless steel plate opposite to the oven nozzle serves as a trap for the nucleobases as well as other components of the residual gas. This way the base pressure during experiments is kept around $1 \times 10^{-8}$ mbar and contributions of the residual gas to the experimental data are negligible.

Two extraction plates located 10 mm apart provide a static electric field of 600 V/cm. To avoid coverage of these plates by adsorbed layers of insulating uracil and particularly thymine, which would distort the homogeneous field, both plates are resistively heated to ≈100°. Due to the electric field, ions generated in the collision region are extracted through a diaphragm and a lens system into a reflectron time-of-flight (TOF) spectrometer (resolution $\Delta m/m = 1500$ at $m = 720$ amu [15]) and detected on a micro sphere plate (MSP) detector. At the same time, electrons are extracted through a 5 mm diaphragm in the positively biased plate and detected on a second MSP detector located behind. A detected electron triggers the TOF measurement and for each such trigger event, several fragment ions can be detected in coincidence (dead time ≈50 ns) and analyzed in an event-by-event mode. Electronically, this is accomplished by using a multi-hit time-to-digital converter (TDC, FAST 7888, 1 ns resolution).

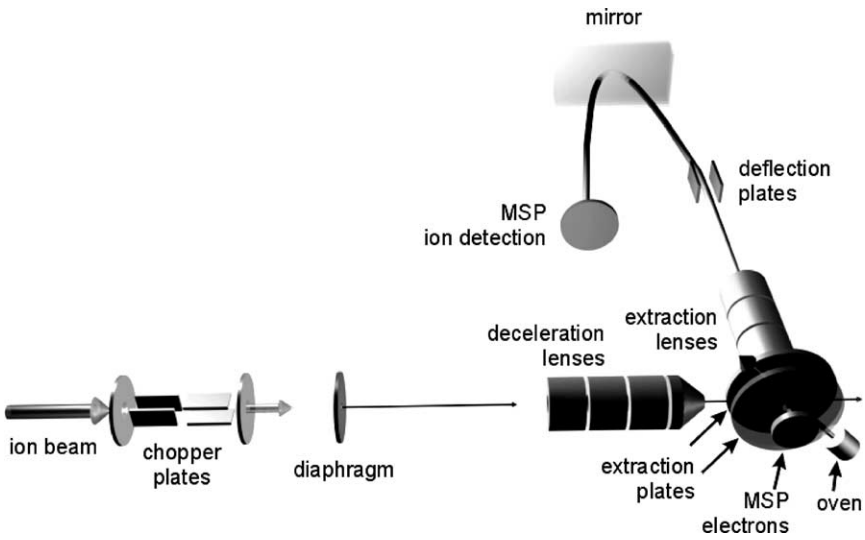


Fig. 2. Sketch of the experimental setup.

## 3. Results and discussion

Typical $m/q$ spectra of the collision products from $^{129}Xe^{25+}$ with uracil and thymine are displayed in Fig. 3. Both spectra show the parent ion peak at $m/q = 112$ and 126 for uracil and thymine respectively. At lower $m/q$, down to about $m/q = 70$, a large gap with no (uracil) or very weak (thymine) peaks is observed. This indicates no (uracil) or almost no (thymine) breakup of the molecules without cleavage of the ring. The groups of peaks down to the $C^+$ peak are each due a fixed number of heavy atoms (C, N, O) with different numbers of H atoms. Patterns like these are typically observed in mass spectrometry of hydrocarbons and it has proven to be difficult to extract information from them. At $m/q$ between 12 and 16 (region "b" in Fig. 3) singly charged atomic ions are found. Lower, between $m/q = 3$ and $m/q = 8$ (region "a"), peaks due to multiply charged atomic ions are observed. Due to the high projectile charge state (25+) and the comparably high projectile velocity $\approx 0.3$ a.u., the intensities of these peaks are comparable to those of the singly charged fragment ion peaks. Furthermore, the maximum charge state is 4, exceeding the values reported previously [14]. (Very recently, Manil et al. [16] studied $Xe^{20+}$ induced fragmentation of the nucleoside (nucleobase + sugar) thymidine from a solid target. Only a weak contribution of atomic ions was observed at all and no multiply charged atomic ions were mentioned in the study. Most probably, the lack of multiply charged atomic ions is due to the solid state of the target, which allows charge and energy dissipation to a large extent.)

The differences between the uracil and the thymine spectra in the low TOF region are negligible. One striking difference is the presence of an $H_2^+$ peak in the case of thymine—a fragment that apparently originates from the methyl-group.

Fig. 4 shows zooms of Fig. 3 regions of multiply charged fragments ("a"). Most of the peaks show a clear splitting due to the fact that only energetic fragments emitted along

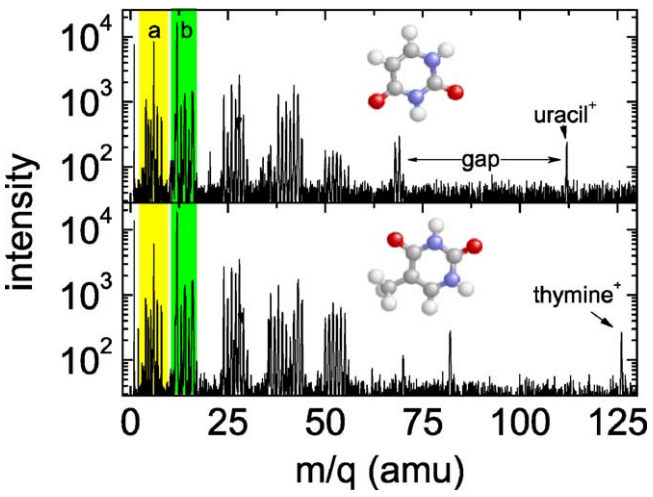


Fig. 3. Electron–ion coincidence TOF spectra of the interaction products from 0.5 MeV $^{129}Xe^{25+}$ with uracil (top) and thymine (bottom).

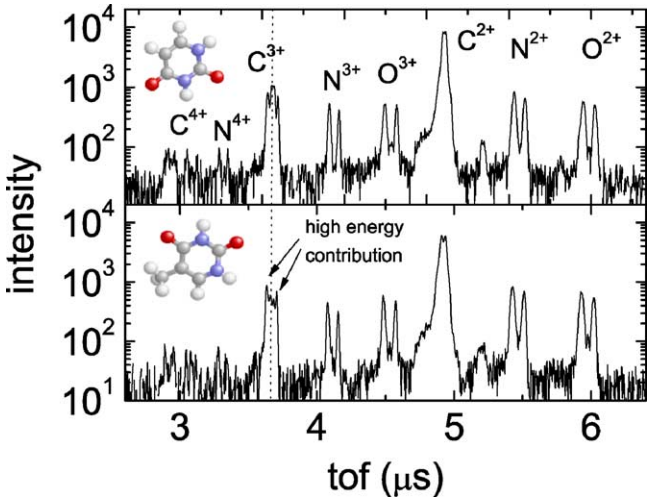


Fig. 4. Zoom into the multiply charged fragment ion region from Fig. 3.

the detection axis are not blocked by the diaphragm in the extraction plate. Those ions emitted towards the detector lead to shorter TOF whereas the ones emitted in the opposite direction have to turn around in the extraction field and are observed at longer TOF. From the time difference $\Delta t$ of both peaks, the kinetic energy of the fragments can be obtained:

$$\Delta t = \frac{2mv_0}{rE} \quad (1)$$

Here, $m$ is the mass of the respective fragment ion, $v_0$ is its initial velocity (due to the fragmentation process), $r$ is the fragment ion charge state and $E$ is the extraction field.

As observed previously for ion induced uracil and thymine fragmentation, peaks due to $C^{r+}$ ions are always stronger than the corresponding $N^{r+}$ and $O^{r+}$ peaks. This is not only due to the larger number of C atoms in the parent molecule. In both molecules, two C atoms originate from sites blocked by an O atom. Coulomb explosion of the multiply charged intermediate complex leaves these $C^{q+}$ ions at relatively low kinetic energies [12,14]. For low energy fragment ions, the transmission to and through the reflectron is close to 100% and thus the corresponding peaks are relatively strong and not split. This is, why in the $C^{3+}/O^{4+}$ peak, the contribution of the latter is expected to be negligible. It is the $C^{3+}$ peak, where the difference between uracil and thymine appears to be most obvious. In the uracil case, even for this relatively highly charged fragment ion, the strongest contribution to $C^{3+}$ is a center peak, (indicated by the dotted line in Fig. 4) due to almost zero kinetic energy ions. In case of thymine, with its additional C atom outside the ring, this center peak is relatively less prominent and higher energy contributions dominate (as indicated in Fig. 4).

By applying Eq. (1) to the TOF spectra from Fig. 4, the kinetic energy distributions of the atomic fragment ions can be calculated. The results are displayed in Fig. 5 for $C^{q+}$, $N^{q+}$ and $O^{q+}$. The displayed data is not corrected for the transmission of the system, since it is non-trivial to obtain the latter: the transmission of the diaphragm in the extraction

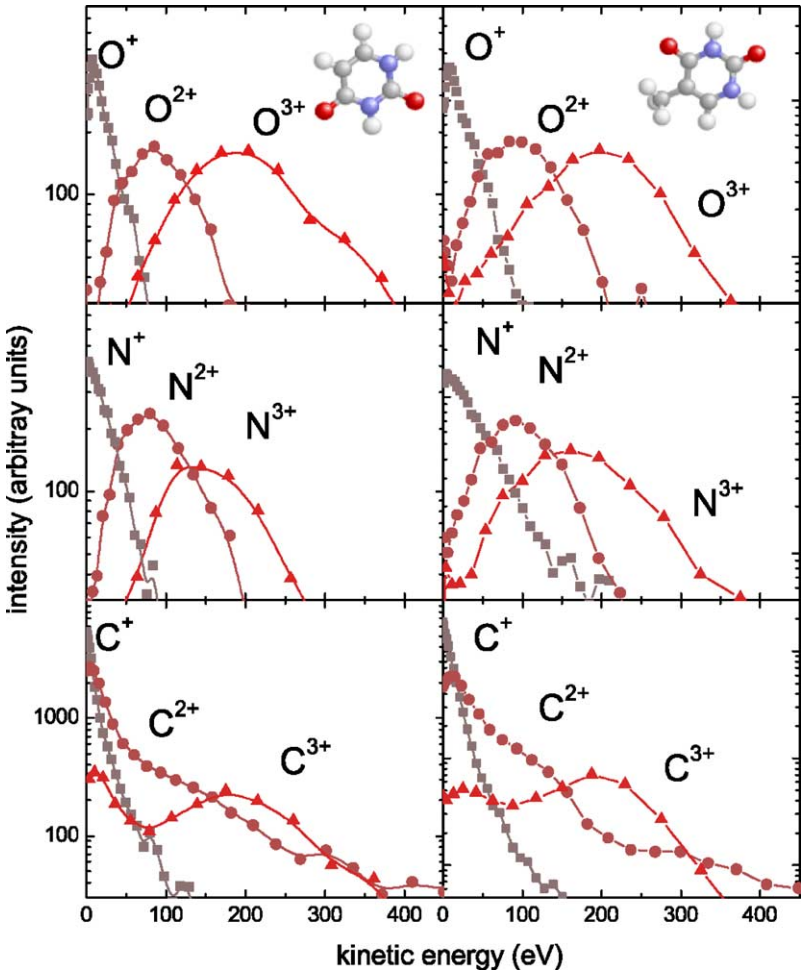


Fig. 5. Kinetic energies of singly and multiply charged atomic fragment ions from uracil (left) and thymine (right) after 0.5 MeV $^{129}Xe^{25+}$ impact.

plate contributes, as well as the transmission of the reflectron itself. Furthermore, the emitted electrons are not necessarily emitted isotropic, neither is their kinetic energy distribution known. Consequently, the transmission of the electrons, which trigger the TOF measurement, is unknown. Fig. 6 displays the transmission curves of $O^{3+}$ ions extracted trough a diaphragm of 5 mm diameter located 5 mm from the collision center (the extraction field was 600 V/cm). Even though the transmission drops fast to values of a few percentage only, for kinetic energies higher than ≈ 50 eV, the curves are relatively flat and do not influence the peak shapes dramatically. Trajectory calculations of the ions within the reflectron revealed that its transmission mimicks the one of a smaller diaphragm. The total transmission is expected to follow a similar curve as Fig. 6, albeit at even lower transmissions.

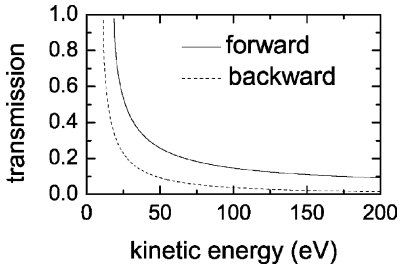


Fig. 6. The transmission functions of the extraction diaphragm for $O^{3+}$ ions emitted towards the detector (forward) and away from it (backward).

The most obvious observation is the similarity of the distributions for uracil and thymine. As already observed from the TOF spectra, the only striking difference is found for $C^{q+}$, in particular for the $C^{3+}$ ions, where two peaks are present in each distribution. Here, in the thymine case fragments have a relatively stronger high energy tail. The peak energies (see Table 1) on the other hand are independent of the parent molecule within the error bars.

Table 1
Most probable kinetic energies (peak positions) of the atomic fragment ions for uracil and thymine (in eV)

| | $C^+$ | $C^{2+}$ | $C^{3+}$ | $N^+$ | $N^{2+}$ | $N^{3+}$ | $O^+$ | $O^{2+}$ | $O^{3+}$ |
|---|---|---|---|---|---|---|---|---|---|
| Uracil | 0 | 0 | 10/175 | 0 | 80 | 144 | 7 | 85 | 185 |
| Thymine | 0 | 0 | 25/185 | 0 | 90 | 161 | 7 | 90 | 195 |

The data have been taken from Fig. 4 and were not corrected for transmission effect. The error is ±8%.

In recent studies on fragment kinetic energies of different aromatic and non-aromatic rings, Coulomb explosion has mainly been induced by short ultrastrong laser-pulses. Shimizu et al. [18] investigated benzene fragmentation upon irradiation with 120 fs/800 nm laser pulses at an intensity of $8 \times 10^{16}$ W/cm$^2$. At such intensities, the obtained TOF spectra of the collision products look similar to our data in the sense, that the singly and doubly charged atomic fragment ion peaks are by far the strongest features in the spectra. At lower laser intensities, singly charged molecular ions become the dominant fragment species (see e.g., [19,20] for fragmentation studies of a variety of aromatic and non aromatic rings at 75 fs/790 nm laser pulses at $2 \times 10^{16}$ to $4 \times 10^{16}$ W/cm$^2$). At higher intensities $\geq 2 \times 10^{17}$ V/cm$^2$, the intensity of the doubly charged species outweightss the singly charged ones and molecular fragments become less important [21].

A typical laser intensity of about $3.6 \times 10^{16}$ W/cm$^2$ corresponds to an electric field of $\approx 5.3 \times 10^9$ V/cm. Approximately the same field is experienced by a target molecule, when a $Xe^{25+}$ ion passes at an impact parameter of 20 a.v. While the field of the ion can be even higher for smaller impact parameters, the field duration at the target molecule location is only a few femtoseconds. In most laser experiments on the other hand, pulses of ≈100 fs duration are used. The longer field–molecule interaction time results into a comparable ionization yield despite the smaller maximum field. In a pioneering study, Mathur [17] compared laser and ion induced fragmentation of benzene and already observed, that the type of field has only a weak influence on the overall fragmentation pattern. However, in that study no data on fragment kinetic energies were presented.

For benzene fragmentation induced by $8 \times 10^{16}$ W/cm$^2$ laser pulses, peak kinetic energies of 20, 60, 85 and 100 eV were later observed for the fragments $C^+$, $C^{2+}$, $C^{3+}$ and $C^{4+}$ [18]. Even though the charge state distribution resembles the results obtained with $Xe^{25+}$ ions, i.e., the number of electrons removed is probably comparable, in the laser case much lower kinetic energies are observed. This is due to the fact, that ionization starts already at the beginning of a pulse, when the electric field is still weak. This ionization initiates the fragmentation process. Later in the evolution of the system, the electric field is sufficient for further ionization, but the molecular constituents already propagated away from their equilibrium distances. The kinetic energies of the fragments reflect the geometry of the intermediate complex with its larger internuclear distances and are thus lower than expected from a simple Coulomb explosion model.

The “half cycle pulse” generated by the passage of a $Xe^{25+}$ ion leads to instant removal of the electrons (compared to the response time of the nuclei) and thus to a Franck–Condon type multiple ionization. The fragment kinetic energies thus reflect the initial geometry of the molecule as well as the initial charge state. To obtain this initial charge state, we performed molecular dynamics calculations of the explosion process of uracil. The code is

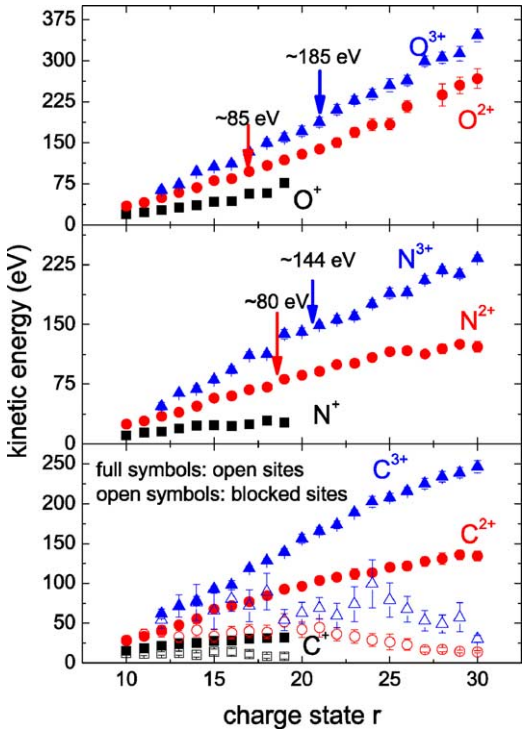


Fig. 7. Simulated fragment ion kinetic energies after removal of $r$ electrons from uracil. The data for $C^{q+}$ ions are split into two sets: one for those ions originating from the blocked sites and the other for those originating from the open sites.

based on the one we developed for simulating the interaction of ions with $C_{60}$ [22]. Here, only the initial geometry reflects the molecular structure. No internuclear forces of the neutral constituents are considered. A fixed number of electrons (10–30) is then removed from the system in a way, that for removal of more than 12 electrons, all constituents are at least singly charged. The remaining electrons are removed in a statistical manner (it is thus averaged over evenly charge distributed configurations as well as configurations with localized charges). The system is then propagated using the Coulomb forces between all constituents until the interionic potentials are negligible. The results of these calculations are displayed in Fig. 7.

As observed experimentally, for the $O^{q+}$ fragment ions which originate from outside the ring, the highest kinetic energies are found. The $N^{q+}$ energies are slightly lower. The $C^{q+}$ data is split into two sets for the ions originating from open (high energies) and from blocked (low energies) sites. As mentioned before, low energy particles have a much higher transmission in our spectrometer and thus readily dominate the experimental results. The low energy contribution is comparable to the $N^{q+}$ data.

Comparing the simulated energies to the experimental data, we can assign most probable initial charge states $r$ of the ionized molecules to the appearance of different fragment ions: Singly charged ions are already produced at charge states much smaller than $r = 10$. $O^{2+}$ corresponds to $r = 17$, $O^{3+}$ to $r = 21$, $N^{2+}$ to $r = 19$ and $N^{3+}$ to $r = 21$.

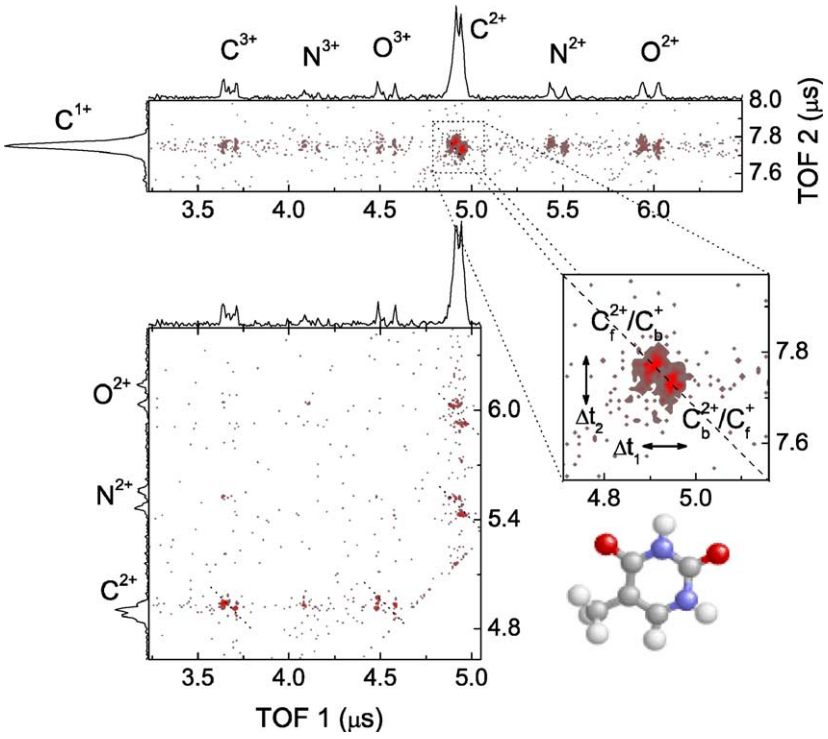


Fig. 8. Electron–ion–ion coincidence plots for thymine fragments after interaction with 0.5 MeV $^{129}Xe^{25+}$. The upper plots shows $C^+$ coincidences with doubly and triply charged fragments (the *Y*-axis is stretched by a factor 2). The lower plot shows coincidences between doubly and triply charged ions. The dotted lines indicate the 45°axis which would occur in case of two body breakup (and momentum conservation).

More detailed information on the fragmentation dynamics can be drawn from electron–ion–ion TOF distributions. Here, for each data point, at least two positively charged fragment ions are detected in coincidence with an electron, serving as a start for the TOF measurement. A resulting coincidence map for thymine fragmentation induced by $^{129}Xe^{25+}$ impact is shown in Fig. 8. Coincidences between ions with identical $m/q$ are supressed because of the dead time of the electronics. The upper plot from Fig. 8 shows coincidences of $C^+$ (*Y*-axis) with doubly and triply charged ions (*X*-axis). For each ion pair, an island shows up in the data. In a two body breakup process, such an island would ideally be rectangularly shaped and conservation of momentum would lead to a −1 slope of the island [23]. In our experiment, only high energy fragments emitted into a small solid angle towards the detector and in the opposite direction pass the diaphragm and the center of the island (the region of small $\Delta t$) vanishes. A typical island thus consists of a contribution due to the first ion being emitted forward (f) and the second ion backward (b) and the other way round (see Fig. 8 for the example of the $C^{2+}/C^+$ island, split into $C_f{}^{2+}/C_b{}^+$ and $C_b{}^{2+}/C_f{}^+$). In many-body fragmentation processes deviations from the −1 slope are expected, since momentum is carried away by undetected fragments. For relatively complex molecules such as thymine and uracil, this can lead to completely different shapes, when e.g., a proton from outside the ring is emitted in the same direction as a heavy fragment [14]. The $C^{2+}/C^+$ island shown in Fig. 8 however, is oriented roughly with a −1 slope. This is most probably due to the fact, that mainly the fragments from the blocked sites with their low kinetic energies contribute. Therefore, the momentum difference of both ions is comparable to the momentum distribution width. In all cases, where the islands are due to a $C^{q+}$ ion together with another species, the slope strongly deviates from −1, again due to the low momentum of the C ions originating from blocked sites.

The $\Delta t$ values obtained from Fig. 8 allow determination of the kinetic energy distribution of the fragment ions for each single island. For instance, from the topmost plot the kinetic energies of $C^{3+}$, $N^{3+}$ and $O^{3+}$ can be obtained for coincidences with $C^+$. From the lower plot, kinetic energies for the same ions in coincidence with $C^{2+}$ can be obtained (in both cases from the projection of the data onto the *X*-axis). Surprisingly, the obtained energies are identical within the error bars, indicating an almost equal initial charge state of the intermediate molecular complex.

## 4. Summary

The Coulomb explosion of the nucleobases uracil and thymine, induced by the strong field of a 0.5 MeV $Xe^{25+}$ ion, has been studied with emphasis on the formation of singly and multiply charged atomic fragment ions. The kinetic energy distributions of these fragments were found to

reflect the geometry of their respective parent molecule. In particular, the results allow to distinguish $C^{q+}$ fragment ions originating from open and blocked sites respectively.

The kinetic energies observed were found to exceed those from Coulomb explosions induced by ultrastrong laser fields of 100 fs pulse length. This can be ascribed to the fact, that the ions can be viewed as "half cycle" pulse of a few femtoseconds which induces a Franck–Condon like multi-ionization process, followed by a Coulomb explosion. In contrast, in the laser case ionization and fragmentation are simultaneous but longer lasting processes and the fragment kinetic energies do not reflect the initial geometry of the molecule.

## Acknowledgements

We gratefully acknowledge financial support from the Stichting voor Fundamenteel Onderzoek der Materie (FOM) which is supported by the Nederlandse Organisatie voor Wetenschapelijk Onderzoek (NWO). TS acknowledges support by the Royal Netherlands Academy of Arts and Sciences. Financial support from the EU network LEIF (HPRI-CT-1999-40012) is gratefully acknowledged.

## References

[1] C. von Sonntag, The Chemical Basis for Radiation Biology, Taylor and Francis, London, 1987.
[2] B.D. Michael, P.D. O'Neill, Science 287 (2000) 1603.
[3] B. Boudaiffa, P. Cloutier, D. Hunting, M.A. Huels, L. Sanche, Science 287 (2000) 1658.
[4] M.A. Huels, I. Hahndorf, E. Illenberger, L. Sanche, J. Chem. Phys. 108 (1998) 1309.
[5] B. Coupier, B. Farizon, M. Farizon, M.J. Gaillard, F. Gobet, V.D. Faria, G. Jalbert, S. Ouaskit, M. Carre, B. Gstir, G. Hanel, S. Denifl, L. Feketeova, P. Scheier, T.D. Märk, Eur. Phys. J. D 20 (2002) 459.
[6] H. Abdoul-Carime, M.A. Huels, F. Brüning, E. Illenberger, L. Sanche, J. Chem. Phys. 113 (2000) 2517.
[7] G. Hanel, B. Gstir, P. Scheier, M. Probst, B. Farizon, M. Farizon, E. Illenberger, T.D. Märk, Phys. Rev. Lett. 90 (2003) 188104.
[8] S. Denifl, S. Ptasinska, M. Cingel, S. Matejcik, P. Scheier, T.D. Märk, Chem. Phys. Lett. 377 (2003) 74.
[9] G. Kraft, Rad. Environ. Biophys. 38 (1999) 229.
[10] G. Kraft, Phys. Med. 17 (2001) 13.
[11] J. de Vries, R. Hoekstra, R. Morgenstern, T. Schlathölter, J. Phys. B: At. Mol. Opt. Phys. 35 (2002) 4373.
[12] J. de Vries, R. Hoekstra, R. Morgenstern, T. Schlathölter, Eur. Phys. J. D 24 (2003) 161.
[13] J. de Vries, R. Hoekstra, R. Morgenstern, T. Schlathölter, Physica Scripta, in press.
[14] J. de Vries, R. Hoekstra, R. Morgenstern, T. Schlathölter, Phys. Rev. Lett. 91 (2003) 053401.
[15] O. Hadjar, R. Hoekstra, R. Morgenstern, T. Schlathölter, Phys. Rev. A 63 (2001) 033201.
[16] B. Manil, H. Lebius, B.A. Huber, D. Cormier, A. Pesnelle, Nucl. Instrum. Meth. B. 205 (2003) 666.
[17] D. Mathur, Phys. Rev. A 63 (2001) 032502.
[18] S. Shimizu, V. Zhakhovskii, F. Sato, S. Okihara, S. Sakabe, K. Nishihara, Y. Izawa, T. Yatsuhashi, N. Nakashima, J. Chem. Phys. 117 (2002) 3180.
[19] P. Tzallas, C. Kosmidis, P. Graham, K.W.D. Ledingham, T. McCanny, S.M. Hankin, R.P. Singhal, P.F. Taday, A.J. Langley, Chem. Phys. Lett. 332 (2000) 236.
[20] P. Tzallas, C. Kosmidis, J.G. Philis, K.W.D. Ledingham, T. McCanny, R.P. Singhal, S.M. Hankin, P.F. Taday, A.J. Langley, Chem. Phys. Lett. 343 (2001) 91.
[21] S. Shimizu, J. Kou, S. Kawato, K. Shimizu, S. Sakabe, N. Nakashima, Chem. Phys. Lett. 317 (2000) 609.
[22] T. Schlathölter, O. Hadjar, J. Manske, R. Hoekstra, R. Morgenstern, Int. J. Mass. Spectrom. 192 (1999) 245.
[23] J.H.D. Eland, F.S. Wort, R.N. Royds, J. El. Spectr. Rel. Phen. 41 (1986) 297.